**Atmospheric
Chemistry
and Physics**
Discussions

Open Access

A 12 year observation of water-soluble inorganic ions in TSP aerosols collected at a remote marine location in the western North Pacific: an outflow region of Asian dust

S. K. R. Boreddy and K. Kawamura

Institute of Low Temperature Science, Hokkaido University, N19, W8, Kita-ku, Sapporo 060-0819, Japan

Correspondence to: K. Kawamura (kawamura@lowtem.hokudai.ac.jp)

ACPD

15, 7419–7458, 2015

A 12 year observation of water-soluble inorganic ions in TSP aerosols

S. K. R. Boreddy and K. Kawamura

Title Page

Abstract	Introduction
Conclusions	References
Tables	Figures

|◀ | ▶|

◀ | ▶

Back | Close

Full Screen / Esc

Printer-friendly Version

Interactive Discussion

S. K. R. Boreddy and K. Kawamura

Abstract

In order to characterize the long term trend of remote marine aerosols, a 12 year observation was conducted for water-soluble inorganic ions in TSP aerosols collected from 2001–2012 in the Asian outflow region at a Chichijima Island in the western North Pacific. We found a clear difference in chemical composition between the continentally affected and marine background air masses over the observation site. Asian continental air masses are delivered from late autumn to spring, whereas marine air masses were dominated in summer. Concentrations of nss-SO_4^{2-}, NO_3^-, NH_4^+, nss-K^+ and nss-Ca^{2+} are high in winter and spring and low in summer. On the other hand, MSA^- exhibits higher concentrations during spring and winter, probably due to springtime dust bloom or due to the direct continental transport of MSA^- to the observation site. We could not find any clear decadal trend for Na^+, Cl^-, Mg^{2+} and nss-Ca^{2+} in all seasons, although there exists a clear seasonal trend. However, concentrations of nss-SO_4^{2-} continuously decreased from 2007–2012, probably due to the decreased SO_2 emissions in East Asia especially in China. In contrast, nss-K^+ and MSA^- concentrations continuously increased from 2001–2012 during winter and spring seasons, demonstrating that biomass burning and/or terrestrial biological emissions in East Asia are increasingly more transported from the Asian continent to the western North Pacific.

1   Introduction

The atmosphere is mostly composed of gases, but also contains suspended liquid and solid particles, called aerosols. Knowledge of the physical and chemical properties of aerosols is important, because of their role in atmospheric processes and climate change. Marine aerosols perturb the earth's radiation balance directly by scattering and absorbing the incoming solar radiation or indirectly by acting as cloud condensation nuclei (CCN) and thus altering their water uptake properties (Twomey, 1977; Charlson et al., 1991; Ramanathan et al., 2001). The strength of these direct and indi-

rect effects depends on the concentration, size distribution, and chemical composition of the atmospheric aerosols (Coakley et al., 1983). In addition, marine aerosols play an important role in atmospheric sulphur cycle of the marine portion (O'Dowd et al., 1997; Faloona, 2009). Thus, meticulous information on the chemical and physical properties of marine aerosol is crucial for the aerosol studies.

Sea salt, ubiquitous and major component in the marine total suspended particulate (TSP) mass has been recognized as the dominant contributor to the clear-sky albedo over the oceans (Haywood et al., 1999). Sea salt aerosols are produced at the ocean surface through the bubble bursting mechanism (Woodcock, 1953). They can affect the chemical and microphysical properties of other aerosol components by taking up and releasing chemically reactive compounds including sulfur and halogen compounds. The sea salt concentration primarily depends on wind speed ranging from 2 to $100 \, \mu g \, m^{-3}$ (Fitzgerald, 1991). Additionally sea salt aerosol particles are hygroscopic by nature (Tang et al., 1997) and hence act as CCN (O'Dowd et al., 1999; Quinn et al., 2000; Ayash et al., 2008).

Non-sea salt (nss-)SO_4^{2-} acts effectively as a reflector of solar radiation and as CCN and, therefore, controls the cloud microphysical properties and cloud albedo (Charlson et al., 1987). The principal source of nss-SO_4^{2-} in the marine atmosphere is the oxidation of gaseous dimethyl sulphide (DMS) emitted by marine phytoplankton (Charlson et al., 1987). Graf et al. (1997) reported that the global burden of nss-SO_4^{2-} (0.78 Tg sulpher) is distributed 37 % from fossil fuel burning, 36 % from volcanoes, 25 % from marine DMS, and 1.6 % from biomass burning. On the other hand, continental anthropogenic nss-SO_4^{2-} and nitrate (NO_3^-) are transported over the remote marine locations and perturb the marine background conditions (Duce and Tindale, 1991; Uematsu et al., 1992; Matsumoto et al., 1998). Methanesulfonate (MSA) is also derived by the oxidation of DMS that originates from the biological activity in the ocean/land (Uematsu et al., 1992; Pavuluri et al., 2011; Miyazaki et al., 2012; Kunwar and Kawamura, 2014).

Anthropogenic and mineral aerosols have significant impact on global climate and also influence the atmospheric chemistry as well as marine ecosystems in remote

oceanic regions (Matsumoto et al., 2004). Bridgman (1990) reported that on average about 185–483 × 10^6 ton global aerosols per year are caused by anthropogenic sources including transportation, stationary combustion, industrial process, solid waste disposal and other miscellaneous sources. East Asia is one of the most swiftly developing re-
⁵ gions in the world and consumes a significant amount of fossil fuels leading to an apparent increase in anthropogenic emission of gaseous pollutants and particulate matter. In addition, high dust loading in spring time is another discernible feature of air quality over the East Asian region (Sun et al., 2001). The long-range atmospheric transport of anthropogenic and mineral aerosols from the Asian continent to the North
¹⁰ Pacific (Kawamura et al., 2003; Matsumoto et al., 2004) and sometimes even North America (Jaffe et al., 2003) by the westerlies may have significant impacts on global radiation balance, atmospheric chemistry, and ocean biogeochemistry (Satheesh and Moorthy, 2005; Rudich et al., 2002; Jickells et al., 2005; Houghton, 2001).

Chichijima Island, a remote marine site in the western North Pacific, is located on
¹⁵ the lee side of a large industrial area and, therefore, this site is well suitable for the study of long-range transport of air pollutants in East Asia and also the perturbation of anthropogenic activity in the remote marine atmosphere. However, the observational data on aerosol chemistry over the western North Pacific are very sparse (Kawamura et al., 2003; Mochida et al., 2003, 2010; Matsumoto et al., 2004; Chen et al., 2013;
²⁰ Boreddy et al., 2014). There is no study on the long term observations of ionic chemical species from the western North Pacific. In order to investigate the annual and seasonal behavior of water-soluble inorganic ions and to clarify decadal trend of the long-range transport of continental aerosols to the remote ocean area, we carried out measurements of atmospheric aerosols at a Chichijima in the western North Pacific.

2 Experimental

2.1 Sampling site and aerosol sampling

Figure 1 shows the sampling location of Chichijima Island in the western North Pacific and its surrounding East Asian regions. This island is about 1000 km from the main Japanese Main Island, Honshu and 2000 km away from the Asian continent. The area within 40 km of this station is covered by oceans and seas. The population of Chichijima is about 2300 and the island's area about 24 km^2 according to the report of the Tokyo metropolitan government bureau of general affairs (http://www.soumu.metro.tokyo.jp/07ogasawara, accessed in November 2011). The observatory is not affected by local pollution, but by the long-range transport of polluted air from the Asian Continent during winter and spring. Therefore the observations at Chichijima Island are useful in discussing the long-range transport of polluted air on a regional scale.

Total suspended particles (TSP) were collected on a weekly basis (4–5 days) at the Satellite Tracking Centre of Japan Aerospace Exploration Agency (JAXA, elevation: 254 m) in Chichijima Island (27°04′ N; 142°13′ E) at a height of 5 m a.g.l. during 2001–2012. Aerosol particles were collected on precombusted (450 °C, 3 h) quartz filters (20 × 25 cm, Pallflex 2500QAT-UP) using a high volume air sampler with a flow rate of 1 m^3 min^{-1} (Kawamura et al., 2003). Filters were placed in a clean glass jar with a Teflon-lined screw cap during the transport and storage. After the sampling, the filters were recovered into the glass jar and stored in a freezer room at −20 °C prior to analysis.

2.2 Analysis of chemical species

All samples were analyzed at Institute of Low Temperature Science, Hokkaido University, Japan. The procedure of chemical analysis is as follows: a punch of 20 mm diameter from each filter sample was extracted with 10 mL organic-free ultrapure wa-

ter (resistivity of $> 18.2\,M\Omega\,cm$, Sartorius arium 611 UV) and ultrasonicated for 30 min. These extracts were the filtrated through a disk filter (Millex-GV, 0.22 µm pore size, Millipore) to remove filter debris and particles and were analyzed for major inorganic ions (MSA^-, Cl^-, SO_4^{2-}, NO_3^-, Na^+, NH_4^+, K^+, Ca^{2+}, and Mg^{2+}) using an ion chromatograph

5 (761 Compact IC, Metrohm, Switzerland).

Major anions were separated on a SI-90 4E Shodex column (Showa Denko, Tokyo, Japan) using a mixture of 1.8 mM Na_2CO_3 + 1.7 mM $NaHCO_3$ solution at a flow rate of 1.2 mL min^{-1} as an eluent and 40 mM H_2SO_4 for a suppressor. For cation measurements, a Metrosep C2-150 (Metrohm) column was used by using a mixture of 4 mM

10 tartaric acid ($C_4H_6O_6$) + 1 mM dipicolinic acid ($C_7H_5NO_4$) solution as eluent at a flow rate of 1.0 mL min^{-1}. The injection loop volume was 200 µL. A calibration curve was evaluated using authentic standards along with a sequence of filter samples. The analytical error in duplicate analysis was about 10 %. Contributions from the field blanks varied between 0–8 and 0–2 % of real samples for anions and cations, respectively,

15 during the sampling period. The concentrations of all inorganic ions reported here are corrected for field blanks that were collected during the sampling period (2001–2012). Total 545 samples were used in this study.

2.3 Synoptic wind pattern and general meteorology

Figure 2 shows monthly mean wind vectors at 850 mb pressure level over Chichijima

20 Island and its surrounding regions, as obtained from the National Centers for Environmental Prediction (NCEP)/National Centre for Atmospheric Research (NCAR) reanalysis (http://www.esrl.noaa.gov/psd/data/gridded/reanalysis/), have been used to ascertain the synoptic conditions during the study period 2001–2012. It is very clear that, from January to April the synoptic winds are stronger, circulation is westerly (from the

25 Asian Continent to the Pacific) and the observation site experiences long-range continental aerosols (anthropogenic and dust). The winds are weakening by May/June and the wind direction changes to southeasterly and continue until August/September.

The observation site gets pristine marine air masses, low wind speed and also much rainfall during southeasterly regime. Again the wind starts shifting from southeasterly to northwesterly/westerly by October and becomes stronger towards December and January–April again. Therefore, on the basis of major synoptic meteorological conditions as above, a year is divided into four seasons: winter (December–February), spring (March–May), summer (June–August) and autumn (September–November) over Chichijima Island.

Based on the historical records from 1974 to 2011 (see Fig. S1 in the Supplement) (http://weatherspark.com/averages/33165/Chichijima-Chichi-Shima-Chubu-Japan), the temperature typically varies from 16–30 °C and is rarely below 13 °C or above 31 °C over the course of a year. In summer, with an average daily high temperature above 28 °C whereas in winter average daily high temperature below 22 °C. The relative humidity typically ranges from 55 % (winter) to 94 % (summer) over the year, rarely dropping below 45 % and reaching as high as 98 %. The highest average wind speed of $4 \, \mathrm{m\,s^{-1}}$ occurs in spring, when the average daily maximum wind speed is $6 \, \mathrm{m\,s^{-1}}$. The lowest average wind speed of $2 \, \mathrm{m\,s^{-1}}$ occurs in summer, when the average daily maximum wind speed is $4 \, \mathrm{m\,s^{-1}}$. In this region, westerly winds dominate in winter to spring and trade winds dominate in summer to autumn.

2.4 Backward air mass trajectories

Figure 3 shows daily 10 day backward air mass trajectories arriving over the observation site, Chichijima at 500 m above the ground level, which were computed for each month using the HYSPLIT model, developed by NOAA/ARL (http://ready.arl.noaa.gov/HYSPLIT.php) (Draxler and Rolph, 2003) during the study period of 2001–2012. In order to assess the influence of long-range transport of air masses as well as the impact of air and sea surface interactions, we chose 500 m altitude in the backward trajectory analysis. The sampling site, Chichijima is located in the western North Pacific in the outflow region of Asian dusts and polluted air masses from China. Therefore, based on the sampling point (JAXA, 254 m a.s.l.) and source regions, we assumed that 500 m

is the minimum altitude to calculate backward air mass trajectories over Chichijima Island. As we discussed above, during winter and spring months, the air masses originate from Siberia passing over Northeast Asia, whereas in the summer months they mostly originate from the Pacific, where pristine air masses exist.

3 Results and discussion

3.1 Evaluation of non sea salt analysis

The contributions from other sources excluding sea salts are calculated using Na^+ as a sea spray marker. However, in this study, for better accuracy, non sea salt components were evaluated from the seasalt (ss) Na^+ fraction (Bowen, 1979; Becagli et al., 2005).

$$nss - SO_4^{2-} = [SO_4^{2-}] - 0.253 \cdot ss - Na^+ \tag{1}$$

$$nss - Ca^{2+} = [Ca^{2+}] - 0.038 \cdot ss - Na^+ \tag{2}$$

$$nss - K^+ = [K^+] - 0.037 \cdot ss - Na^+ \tag{3}$$

where $[SO_4^{2-}]$, $[Ca^{2+}]$ and $[K^+]$ are the total measured TSP mass concentrations and ss-Na^+ was calculated using the four equation system reported below and knowing total Na^+, total Ca^{2+}, the mean Ca^{2+}/Na^+ ratio in the crust $((Na^+/Ca^{2+})_{crust} = 1.78\,\text{w/w}$; Bowen, 1979) and the mean Ca^{2+}/Na^+ ratio in sea water $((Ca^{2+}/Na^+)_{seawater} = 0.038\,\text{w/w}$; Bowen, 1979).

$$ss - Na^+ = Na^+ - nss - Na^+$$

$$nss - Na^+ = nss - Ca^{2+} \cdot (Na^+/Ca^{2+})_{crust}$$

$$nss - Ca^{2+} = Ca^{2+} - ss - Ca^{2+}$$

$$ss - Ca^{2+} = ss - Na^+ \cdot (Ca^{2+}/Na^+)_{seawater} \tag{4}$$

Crustal contribution to water-soluble sodium was estimated to be 0.004–0.94 with a mean of 0.078 ± 0.071 during the study period at Chichijima Island.

3.2 Ion balance

In order to assess the quality of the analysis we performed an ion balance calculation, using major anions (Cl^-, SO_4^{2-}, NO_3^-) and cations (Na^+, NH_4^+, K^+, Ca^{2+}, and Mg^{2+}) assuming that most of the ions are in the solutions. Based on the electroneutrality principle, the sum of total anions ($\mu eq\, m^{-3}$) should be equal to the sum of total cations ($\mu eq\, m^{-3}$) in the solutions and this ratio is a good indicator to study the acidity of aerosols over the sampling site. The following equations are used here to calculate the charge balance between cations and anions.

$$\text{Cation equivalent } (\Sigma^+) = \frac{Na^+}{23} + \frac{NH_4^+}{18} + \frac{K^+}{39} + \frac{Mg^{2+}}{12} + \frac{Ca^{2+}}{20} \qquad (5)$$

$$\text{Anion equivalents } (\Sigma^-) = \frac{SO_4^{2-}}{48} + \frac{NO_3^-}{62} + \frac{Cl^-}{35.5} \qquad (6)$$

The relationship between anions and cations for different seasons are shown in Fig. 4. We found that correlation coefficients of anion vs. cation were higher than 0.92 for all seasons, which represent a good quality of data and also indicate that ions share a common origin (Zhang et al., 2011). The slopes of linear regression lines for the seasonally stratified data are > 1 with the following order: summer (1.264) > spring (1.256) > autumn (1.252) > winter (1.231). This result suggests that in all seasons, the TSP was apparently acidic. As most of the major ions were measured except for hydrogen ions (H^+), the cation deficits are probably due to H^+ ion.

3.3 Temporal variations of major inorganic species, $MSA^-/nss\text{-}SO_4^{2-}$ and Σ^-/Σ^+ ratios

Figure 5 presents temporal variations of major inorganic ions, $MSA^-/nss\text{-}SO_4^{2-}$ and Σ^-/Σ^+ ratios for the period 2001–2012 over the sampling site. All the measured ions showed a clear temporal trend for each year during the study period. The Σ^-/Σ^+ ratio ($\mu eq\,m^{-3}$), which is a good indicator of acidity of aerosols over the environment, ranged from 0.8 to 1.6 with a mean of 1.2 ± 0.1, demonstrating that aerosol particles are acidic over Chichijima Island (Fig. 5a). The $MSA^-/nss\text{-}SO_4^{2-}$, which can be used as a tracer to assess the contribution of biogenic sources to sulfate in the atmosphere (Savoie and Prospero, 1989), varied between 0.002 and 0.064 with a mean of 0.014 ± 0.01 and summertime maxima (Fig. 5b).

Sea salt species (Cl^- and Na^+) are found as the most abundant ranging from 0.92 to $16.6\,\mu g\,m^{-3}$ with a mean of $6.31 \pm 2.61\,\mu g\,m^{-3}$ and from 0.61 to $7.36\,\mu g\,m^{-3}$ with a mean of $3.39 \pm 1.20\,\mu g\,m^{-3}$, respectively (see Fig. 5i and k). Concentrations of $nss\text{-}SO_4^{2-}$ varied from 0.09 to $7.85\,\mu g\,m^{-3}$ with a mean of $2.17 \pm 1.53\,\mu g\,m^{-3}$ (see Fig. 5e) whereas those of nitrate ranged from 0.09 to $1.17\,\mu g\,m^{-3}$ (mean $0.57 \pm 0.37\,\mu g\,m^{-3}$). Although NH_4^+ was less abundant throughout the sampling period, we found significant levels under the influence of continental air masses in the spring. Its concentrations ranged from 0.01 to $1.10\,\mu g\,m^{-3}$ with a mean of $0.17 \pm 0.16\,\mu g\,m^{-3}$ (Fig. 5h). Concentrations of MSA^-, a marker of biogenic source, varied from 0.006 to $0.055\,\mu g\,m^{-3}$ with a mean of 0.021 ± 0.009 (Fig. 5f). $Nss\text{-}Ca^{2+}$ ($nss\text{-}K^+$), a tracer for dust (biomass burning), ranged from 0.002 to $0.84\,\mu g\,m^{-3}$ (0.002 to $0.19\,\mu g\,m^{-3}$) with a mean of $0.13 \pm 0.15\,\mu g\,m^{-3}$ ($0.04 \pm 0.03\,\mu g\,m^{-3}$) (Fig. 5c, 5d). Concentrations of Mg^{2+} ranged from 0.06 to $0.78\,\mu g\,m^{-3}$ with a mean of $0.40 \pm 0.14\,\mu g\,m^{-3}$ (Fig. 5j). It is also noteworthy that the sum of all the water-soluble inorganic ions (WSIM) ranged from 2.9 to $25.7\,\mu g\,m^{-3}$ with a mean of $13.1 \pm 4.8\,\mu g\,m^{-3}$ in Chichijima TSP aerosols for the study period of 2001–2012 (not shown as a figure).

3.4 Monthly variations of major inorganic species and $MSA^-/nss\text{-}SO_4^{2-}$

Figure 6 gives Box–Whisker diagrams of monthly variations of different chemical species at Chichijima Island in the western North Pacific for the period of 2001–2012. Almost all the ions showed a clear monthly/seasonal variation with higher concentra-
5 tions during the long-range atmospheric transport of continental air mass and lower concentrations under the influence of marine air mass. Seasonal and annual mean concentrations of major inorganic ions (mean ± SD) and the two tailed P value for the study period (2001–2012) were reported in Tables 1 and 2, respectively. These seasonal and annual differences are verified by t test. The t test results show that these
10 differences are statistically significant with two tailed P values of less than 0.001.

As illustrated in Fig. 6a and b, sea salt particles are characterized by a gradual increase from autumn to winter, with a peak in early spring (March). Thereafter, Na^+, Cl^- minimized in early summer (June) and again increased toward winter. We found the significantly high concentration during August; probably due to the influence of
15 southeast Asian air masses (see Fig. 3). This trend of sea salts is similar to that of wind speed over the sampling site; that is, higher wind speeds during spring/winter and lower in the summer. This result suggests that the concentrations of sea salt are mainly depends on wind speed. It is also worthy to note that the similar seasonal pattern can also be seen in the concentrations of Mg^{2+} (see Fig. 6c), indicating that Mg^{2+}
20 comes from the ocean rather continental sources. This is further supported by the existing correlation between Mg^{2+} and Na^+. We found a strong correlation ($R^2 = 0.94$ and slope = 0.117) between Mg^{2+} and Na^+ with the ratio being very close to seawater (0.12).

The seasonal variations of NH_4^+ and NO_3^- are characterized by spring maxima and
25 summer minima. NH_4^+ concentrations are low throughout the sampling period over the Chichijima Island (Fig. 6d and e), probably because the sampling site is far away from the source regions of ammonia over the Asian continent (Boreddy et al., 2014; Matsumoto et al., 2007). The residence time of NH_3 is around several hours in the marine

boundary layer (Quinn et al., 1990) and the concentration of NH_3 transported from continental to remote marine locations should be considerably low. Interestingly, we found a significantly higher concentration of NO_3^- than that of NH_4^+ over the sampling site, which may result from some additional NO_3^- sources. The heterogeneous reaction,

5 $HNO_3 + NaCl \rightarrow NaNO_3$, can provide an additional source of NO_3^- in TSP aerosols (Wu et al., 2006) over the observation site. Further, the low temperature over East Asian regions in winter and spring would favor the shift from the gas phase of nitric acid to nitrate in the particle phase, which could lead to higher concentration of NO_3^- that is transported to the western North Pacific in winter and spring. On the other hand, nss-

10 K^+ that is derived mainly from biomass burning was also quite low in Chichijima TSP aerosols, although it shows a higher concentration in winter and spring than in summer and autumn. The seasonal variation of nss-SO_4^{2-} showed maxima in the spring/winter and minima in summer (see Fig. 6h), being similar to that of NO_3^-. This result indicates that the higher levels of nss-K^+ during the winter and spring mainly associated with the

15 long-range atmospheric transport of anthropogenic/biomass burning particles over the observation site.

The concentrations of nss-Ca^{2+} drastically increased in spring when the Asian dusts were transported over the observation site by westerly winds (see Fig. 6i). This result is consistent with the previous studies (Kawamura et al., 2003; Suzuki et al., 2008;

20 Guo et al., 2011) where nss-Ca^{2+} maximized in spring. A strong seasonal variability was found in MSA^- concentrations with higher values in spring followed by winter and lower values in autumn and summer. This strong seasonal variability in MSA^- can be ascribed to seasonality of photochemistry, biology, and meteorology. It is worth noting that the mass concentration of MSA^- showed similar seasonal variation with nss-Ca^{2+}

25 and NO_3^-, although its concentrations are much lower than that of nss-Ca^{2+} and NO_3^-. This result suggests that there should be a link between dust and biological emissions and NO_3 radicals (see Fig. 6g). This point will be discussed in more details in the subsequent sections. The mass ratio MSA^-/nss-SO_4^{2-} showed a clear, distinct variation characterized by a gradual increase from winter to spring with a peak in summer. It

again gradually decreased toward winter (see Fig. 6f). This result illustrates that the contribution of marine biogenic sources to nss-SO_4^{2-} was higher in summer, because of higher solar radiation that enhances the biological activity over the sampling site. We also found co-variation between MSA^-/nss-SO_4^{2-} ratio and air temperature, both of which showed maxima in summer followed by spring and minima in winter.

3.5 Annual variations of different chemical species on a seasonal scale

Figure 7 presents the annual variations of selected chemical species for different seasons in the period of 2001–2012. Although there exist some seasonal trends of ions, we couldn't find any clear annual trends for the species Cl^-, Mg^{2+} and nss-Ca^{2+} in all seasons. However, nss-SO_4^{2-} and NO_3^- showed a clear annual trend for all seasons, with an increase from 2001–2004 and decrease from 2007–2012. Lu et al. (2010) reported that total SO_2 emission in China increased by 53 % (21.7–33.2 Tg, at an annual growth rate of 7.3 %) from 2000 to 2006, during which emissions from power plants are the main sources of SO_2 in China with an increase from 10.6 to 18.6 Tg per year. Geographically, emission from north China increased by 85 %, whereas that from the south increased by only 28 %. The growth rate of SO_2 emission slowed down around 2005, and began to decrease after 2006 mainly due to the wide operation of flue-gas desulfurization (FGD) devices in power plants in response to a new policy of Chinese government. This change in the SO_2 emissions was exactly recorded in our observation at Chichijima in the western North Pacific, that is, the decreasing trend of SO_4^{2-} concentrations over the observation site can be explained by the decrease in SO_2 emissions in China after 2006. Further, these results are supported by the annual variation of nss-SO_4^{2-}/Na^+ and nss-NO_3^-/Na^+ mass ratios (see Fig. 7j and k). The nss-SO_4^{2-}/Na^+ ratio showed a clear annual trend in winter and spring with an increase from 2001 to 2004 and decreasing trend from 2007 to 2012. Therefore, nss-SO_4^{2-} concentrations in the western North Pacific are gradually decreasing, because of the suppressed emission of SO_2 over East Asia, especially in China.

In contrast, the annual variation of nss-K$^+$ showed an increasing trend from 2001 to 2004 and 2006 to 2012, suggesting that biomass burning emissions in East Asia are continuously increasing and transported to the western North Pacific by long-range atmospheric transport. This result is further supported by the study of Verma et al. (2014) (submitted to JGR), who reported long term measurements of biomass burning organic tracers (levoglucosan, mannosan and galactosan) for the period of 2001–2013 over the same observation site, Chichijima Island. They found a continuous increase in the concentrations of biomass burning tracers from 2006 to 2013, which is mainly caused by enhanced biomass burning in East Asia. It is of interest to note that the annual variation of MSA$^-$ concentrations have shown a gradual increase from 2001 to 2012 during the winter and spring seasons, indicating that direct transport of MSA$^-$ from the continental surface to the remote marine locations is continuously increasing. On the other hand, NH$_4^+$ concentrations showed a gradual decrease from 2006 to 2012 during winter and spring seasons, whereas in summer and autumn, we couldn't find any clear annual trends in the abundance of NH$_4^+$.

3.6 Correlation analyses among the inorganic ions

In order to extract the crucial information about the sources of ions, we performed a correlation analysis among the ions for different seasons. Table 3 shows the results of correlation analyses of major ions for winter, spring, summer, and autumn during the study period. In all seasons, we found strong correlations (excellent correlation during summer and autumn) among Na$^+$, Mg^{2+}, and Cl$^-$, indicating that these ions are mainly derived from sea spray. Although NH$_4^+$ concentrations are low throughout the campaign period, they show a good correlation with SO$_4^{2-}$ during all seasons. NH$_4^+$ should be present as (NH$_4$)$_2$SO$_4$ or NH$_4$HSO$_4$ in aerosols.

During winter, nss-K$^+$, a tracer of biomass burning, strongly correlates with nss-SO$_4^{2-}$. This result suggests that they are derived from continental sources including biomass burning and fossil fuel combustion. In contrasts, NO$_3^-$, a tracer of anthropogenic source,

correlates with NH_4^+, Na^+, and nss-K^+ with a relatively strong correlation coefficient ($r > 0.55$), suggesting that they are derived from biomass burning and anthropogenic sources in the Asian continent. In spring, Ca^{2+} strongly correlate with NO_3^- ($r = 0.62$) and moderately correlate with Mg^{2+}, nss-K^+, and nss-SO_4^{2-}, indicating that they are derived from similar sources or reaction pathways. It is important to note that Na^+ moderately correlated with NO_3^- and SO_4^{2-} during spring, whereas no correlation was found in summer, suggesting that chloride loss is prominent in spring compared to summer. HNO_3 probably reacts with sea salt and dust particles in the marine atmosphere.

$$HNO_3 + NaCl \rightarrow NaNO_3 + HCl(\uparrow) \tag{7}$$

$$2HNO_3 + Ca \rightarrow Ca(NO_3)_2 + H_2(\uparrow) \tag{8}$$

3.7 Percent contribution of major ions to total WSIM

The percent contributions of individual inorganic species to the total WSIM are shown as a pie chart in Fig. 8 for the different seasons. Among all the inorganic species, sea salt (NaCl) is a major contributor to the WSIM, followed by nss-SO_4^{2-} and NO_3^- during all seasons. Na^+ and Cl^- together contributed ~ 70, 66, 80 and 82 % to the total WSIM for winter, spring, summer and autumn, respectively, whereas nss-SO_4^{2-} contributed ~ 26, 24, 11 and 10 %, respectively. The nss-Ca^{2+} shows a significant contribution (about 2 %) to WSIM in spring, indicating a long-range atmospheric transport of Asian dusts over the observation site. Similarly, Mg^{2+} contributed to the total WSIM by about 3 % in all seasons.

We found a significant depletion of chloride during winter and spring, probably due to the atmospheric mixing of anthropogenic pollutants such as SO_2, NO_3, etc. (Boreddy et al., 2014a). Figure 9a and b shows the monthly and seasonal variations of Cl^-/Na^+ mass ratio during the study period. The monthly-averaged Cl^-/Na^+ ratio varied from 1.58 to 2.05 with a mean value of 1.79 ± 0.15. Although the mean mass ratio is almost equal to that of seawater (1.8), we found significant chlorine loss in the winter and spring samples. Atmospheric processing of anthropogenic pollutants/minerals and their

mixing with sea salt particles during the long-range atmospheric transport are probably responsible for the chlorine loss. On the other hand acid displacement also plays an important role in chloride depletion over the marine environment through the following reactions,

$$2NaCl + H_2SO_4 \rightarrow Na_2SO_4 + 2HCl \tag{9}$$

Further, Mochida et al. (2003) reported high abundance of oxalic acid in the Chichi-jima TSP aerosols in spring. Oxalic acid may be internally mixed with dust-derived minerals. Previous studies of Asian dust showed that oxalate was largely mixed with dust particles (Sullivan and Prather, 2007). Therefore, it is reasonable to assume that the spring time chlorine loss over the western North Pacific was most likely due to the displacement of Cl^- with oxalate through the following reaction,

$$2NaCl + H_2C_2O_4 \rightarrow Na_2C_2O_4 + 2HCl \tag{10}$$

In contrast, during the summer and autumn, we found an excess of chloride over the observation site, because of some additional source of chloride added to the TSP aerosols.

3.8 Which biological source is more important as a contributor to MSA^-?

To better identify the biological source as a more significant contribution to MSA^-, we compared the monthly mean variation of MSA^- with chlorophyll a (Chl a ($mg\,m^{-3}$), a satellite derived biogenic tracer) during the study period as shown in Fig. 10. Chl a concentrations were downloaded from MODIS AQUA satellite over the region of 140–145° E, 25–30° N for the period July 2002–December 2012. We found a clear monthly/seasonal variation in Chl a concentration, which gradually increased from autumn to early spring and then decreased from mid spring to summer. Surprisingly, similar seasonal pattern can also be seen in the concentrations of nss-Ca^{2+} (see Fig. 6i), indicating that there should exist a possible link between the long-range transport of

A 12 year observation of water-soluble inorganic ions in TSP aerosols

S. K. R. Boreddy and K. Kawamura

Asian dusts (or a springtime bloom) and the ocean productivity in the western North Pacific. The production of algal blooms may quickly respond to dust deposition (nutrients) over the surface ocean (Gabric et al., 2004). By changing the phytoplankton productivity, dusts can act as important source of DMS production (Jickells et al., 2005). However, the mechanisms of marine phytoplankton response to a dust input from the atmosphere are still facing with numerous uncertainties, a subject of scientific discussion.

Ramos et al. (2005) observed the massive Saharan dust storms along with algal bloom observed in the north Atlantic in August 2004. Bishop et al. (2002) observed an increase in chlorophyll *a* over a couple of weeks in the North Pacific after passage of Gobi desert dust cloud. Springtime bloom in the north East China Sea and Japan Sea was observed by TOMS and SeaWiFS satellites to be initiated one month earlier than usual, being correlated with an Asian dust event in association with precipitation. Such event leads to a supply of bioavailable iron and to induce a deepening of the critical depth, which results in an early initiation of the bloom (Jo et al., 2007). On the other hand, Gabric et al. (2004) revealed that the dust storms in Australia (2002–2003) lead to advection of large dust plumes over the Southern Ocean, and observed a coherence between optical characteristics of the Southern Ocean atmosphere and dust loading by satellite and field data on surface ocean chlorophyll *a*. Therefore, it is noteworthy that the transported atmospheric dust particles can act as a fertilizer to stimulate the production of microscopic marine plants (plankton/algae blooms).

As discussed in Sect. 3.4, the monthly variation of MSA^- gradually increased from winter to spring, with a peak in April and gradually decreased towards summer and autumn months. Interestingly, MSA^- maximized in April whereas chlorophyll *a* maximized in March, although both are tracers for the marine biological activity. It is also important to mention that the highest concentration of MSA^- was observed one month after the Asian dust deposition over the ocean surface, suggesting that there may be a time lag between the dust deposition and DMS emissions. Therefore, we assume that there are two possible sources for higher MSA^- concentrations in winter/spring

over the Chichijima island, (1) direct transport of MSA⁻ from the continental sources, such as industrial emissions (Lu et al., 2010), terrestrial higher plants (Pavuluri et al., 2013), and forest floors (Miyazaki et al., 2012), and (2) springtime bloom of phytoplankton over the western North Pacific.

⁵   Another factor that could affect MSA concentrations is concentrations of NO_3 radicals, which are among the key oxidants for MSA production. Polluted air mass with higher NO_x concentrations gives higher MSA yields relative to SO_2 from DMS oxidation (Yin et al., 1990). Under prevailing westerly polluted winds, significant amount of anthropogenic NO_x can be transported from East Asia over the western North Pacific, ¹⁰ which could enhance the MSA concentrations relative to the less polluted pristine air masses. Similar results are reported elsewhere (Yin et al., 1990; Jensen et al., 1991; Mihalopoulos et al., 1992; Gao et al., 1996). Further, temperature is also an important factor to control the MSA⁻ concentrations through the mechanism of DMS oxidation by hydroxyl radicals (Arimoto et al., 1996). In the present study, we found lower con- ¹⁵ centrations of MSA⁻ during summer and autumn months when ambient temperature is higher, demonstrating that lower temperature may lead to higher MSA concentration in this region. However, the MSA concentrations in the marine atmosphere could be affected by multiple processes relating to primary productivity, such as spatial variability of phytoplankton species, air–sea exchange rates of DMS, and different oxidation ²⁰ pathways of DMS. In addition, variations in environmental conditions such as temperatures, precipitation patterns, sea-ice conditions, winds and ocean currents could also control the concentrations of MSA (Gao et al., 1996).

4 Summary and conclusions

We conducted 12 year observation of water-soluble inorganic ions in TSP aerosols, ²⁵ from the remote marine location, Chichijima Island, in the western North Pacific. Long-term observation of marine aerosols provides the following findings.

1. Water-soluble inorganic ions in the TSP aerosols are dominated by sea salt particles (Na^+ and Cl^-), which contributed about 75 % to the total WSIM followed by anthropogenic species such as nss-SO_4^{2-}, and NO_3^-.

2. Sea salt components showed prominent peaks in autumn and winter months and minimized in spring and summer probably due to the variations in wind speed over the observation site. nss-SO_4^{2-}, NO_3^-, and nss-K^+ showed higher concentrations in winter and spring, due to the atmospheric long-range transport of anthropogenic pollutants and biomass burning emissions in East Asia. Although NH_4^+ concentrations are relatively low throughout the sampling period over the Chichijima Island, they showed prominent peaks in spring and winter months. The concentrations of nss-Ca^{2+} in TSP drastically increased in spring when the Asian dusts are delivered to the observation site.

3. Interestingly, concentrations of nss-SO_4^{2-} during winter and spring decreased from 2007 to 2012 probably due to the decrease in SO_2 emissions in China after 2006. A similar trend was seen in the concentrations of NO_3^- during the study period. In contrast, the concentration of nss-K^+ showed continuous increase from 2001 to 2004 and 2006 to 2012, suggesting that biomass burning emissions in East Asia are more increased followed by the atmospheric transporte to the western North Pacific. On the other hand, MSA^- concentrations during winter to spring continuously increased from 2001 to 2012, indicating that direct continental transport of Asian dust followed by springtime bloom in the ocean play an important role on the annual variation of MSA^- concentrations over the western North Pacific.

4. We also found there is a time lag between the measured concentration of MSA^- in the aerosols and satellite derived biological tracer (chlorophyll *a*), suggesting that variability of phytoplankton, sea–air exchange rate of DMS emissions, and other environmental conditions can play an important role in controlling the concentrations of MSA^- over the observation site.

Title Page

Abstract | Introduction

Conclusions | References

Tables | Figures

|◄ | ►|

◄ | ►

Back | Close

Full Screen / Esc

Printer-friendly Version

Interactive Discussion

References

Arimoto, R., Duce, R. A., Savoie, D. L., Prospero, J. M., Talbot, R., Cullen, J. D., Tomza, U., Lewis, N. F., and Ray, B. J.: Relationships among aerosol constituents from Asia and the North Pacific during PEM-West A, J. Geophys. Res.-Atmos., 101, 2011–2023, doi:10.1029/95JD01071, 1996.

Ayash, T., Gong, S., and Jia, C. Q.: Direct and indirect shortwave radiative effects of sea salt aerosols, J. Climate, 21, 3207–3220, 2008.

Bishop, J. K. B., Davis, R. E., and Sherman, J. T.: Robotic observations of dust storm enhancement of carbon biomass in the North Pacific, Science, 298, 817–821, 2002.

Boreddy, S. K. R., Kawamura, K., and Jung, J. S.: Hygroscopic properties of particles nebulized from water extracts of aerosols collected at Chichijima Island in the western North Pacific: an outflow region of Asian dust, J. Geophys. Res.-Atmos., 119, 167–178, doi:10.1002/2013jd020626, 2014.

Bridgman, H. A.: Global Air Pollution: Problems for the 1990s, Belhaven Press, 25 Floral Street, London WCzzz2E, 9DS, 1990.

Charlson, R. J., Lovelock, J. E., Andreae, M. O., and Warren, S. G.: Oceanic phytoplankton, atmospheric sulphur, cloud albedo and climate, Nature, 326, 655–661, 1987.

Charlson, R. J., Langner, J., Rodhe, H., Leovy, C. B., and Warren, S. G.: Perturbation of the Northern-Hemisphere radiative balance by backscattering from anthropogenic sulfate aerosols, Tellus A, 43, 152–163, 1991.

Chen, J., Kawamura, K., Liu, C.-Q., and Fu, P.: Long-term observations of saccharides in re-
mote marine aerosols from the western North Pacific: a comparison between 1990–1993 and
2006–2009 periods, Atmos. Environ., 67, 448–458, doi:10.1016/j.atmosenv.2012.11.014,
2013.

5 Coakley, J. A., Cess, R. D., and Yurevich, F. B.: The effect of tropospheric aerosols on the Earths
radiation budget – a parameterization for climate models, J. Atmos. Sci., 40, 116–138, 1983.

Draxler, R. R. and Rolph, G. D.: HYSPLIT (HYbrid Single-Particle Lagrangian Integrated Trajec-
tory) Model, access via NOAA ARL READY Website, available at: http://www.arl.noaa.gov/
ready/hysplit4.html (last access: July 2013), NOAA Air Resources Laboratory, Silver Spring,

10 MD, 2003.

Duce, R. A. and Tindale, N. W.: Atmospheric transport of iron and its deposition in the ocean,
Limnol. Oceanogr., 36, 1715–1726, 1991.

Faloona, I.: Sulfur processing in the marine atmospheric boundary layer: a review and critical
assessment of modeling uncertainties, Atmos. Environ., 43, 2841–2854, 2009.

15 Fitzgerald, J. W.: Marine aerosols – a review, Atmos. Environ. A-Gen., 25, 533–545, 1991.

Gabric, A. J., Simo, R., Cropp, R. A., Hirst, A. C., and Dachs, J.: Modeling estimates of the global
emission of dimethylsulfide under enhanced greenhouse conditions, Global Biogeochem.
Cy., 18, GB2014, doi:10.1029/2003GB002183, 2004.

Gao, Y., Arimoto, R., Duce, R. A., Chen, L. Q., Zhou, M. Y., and Gu, D. Y.: Atmospheric non-

20 sea-salt sulfate, nitrate and methanesulfonate over the China Sea, J. Geophys. Res.-Atmos.,
101, 12601–12611, doi:10.1029/96JD00866, 1996.

Graf, H. F., Feichter, J., and Langmann, B.: Volcanic sulfur emissions: estimates of source
strength and its contribution to the global sulfate distribution, J. Geophys. Res.-Atmos., 102,
10727–10738, 1997.

25 Guo, Y.-T., Zhang, J., Wang, S.-G., She, F., and Li, X.: Long-term characterization of major
water-soluble inorganic ions in PM_{10} in coastal site on the Japan Sea, J. Atmos. Chem., 68,
299–316, doi:10.1007/s10874-012-9223-8, 2011.

Haywood, J. M., Ramaswamy, V., and Soden, B. J.: Tropospheric aerosol climate forcing in
clear-sky satellite observations over the oceans, Science, 283, 1299–1303, 1999.

30 Houghton, J. T., Ding, Y., Griggs, D. J., Noguer, M., van der Linden, P. J., Dai, X., Maskell, K.,
Johnson, C. A.: Climate Change 2001: The Scientific Basis, Cambridge University Press,
Cambridge, 2001.

Jaffe, D., McKendry, I., Anderson, T., and Price, H.: Six "new" episodes of trans-Pacific transport of air pollutants, Atmos. Environ., 37, 391–404, doi:10.1016/S1352-2310(02)00862-2, 2003.

Jensen, N. R., Hjorth, J., Lohse, C., Skov, H., and Restelli, G.: Products and mechanism of the reaction between NO_3 and dimethylsulphide in air, Atmos. Environ. A-Gen., 25, 1897–1904, doi:10.1016/0960-1686(91)90272-9, 1991.

Jickells, T. D., An, Z. S., Andersen, K. K., Baker, A. R., Bergametti, G., Brooks, N., Cao, J. J., Boyd, P. W., Duce, R. A., Hunter, K. A., Kawahata, H., Kubilay, N., laRoche, J., Liss, P. S., Mahowald, N., Prospero, J. M., Ridgwell, A. J., Tegen, I., and Torres, R.: Global iron connections between desert dust, ocean biogeochemistry, and climate, Science, 308, 67–71, doi:10.1126/science.1105959, 2005.

Jo, C. O., Lee, J. Y., Park, K. A., Kim, Y. H., and Kim, K. R.: Asian dust initiated early spring bloom in the northern East/Japan Sea, Geophys. Res. Lett., 34, L05602, doi:10.1029/2006GL027395, 2007.

Kawamura, K., Ishimura, Y., and Yamazaki, K.: Four years' observations of terrestrial lipid class compounds in marine aerosols from the western North Pacific, Global Biogeochem. Cy., 17, 1003, doi:10.1029/2001GB001810, 2003.

Kunwar, B. and Kawamura, K.: One-year observations of carbonaceous and nitrogenous components and major ions in the aerosols from subtropical Okinawa Island, an outflow region of Asian dusts, Atmos. Chem. Phys., 14, 1819–1836, doi:10.5194/acp-14-1819-2014, 2014.

Lu, Z., Streets, D. G., Zhang, Q., Wang, S., Carmichael, G. R., Cheng, Y. F., Wei, C., Chin, M., Diehl, T., and Tan, Q.: Sulfur dioxide emissions in China and sulfur trends in East Asia since 2000, Atmos. Chem. Phys., 10, 6311–6331, doi:10.5194/acp-10-6311-2010, 2010.

Matsumoto, K., Nagao, I., Tanaka, H., Miyaji, H., Iida, T., and Ikebe, Y.: Seasonal characteristics of organic and inorganic species and their size distributions in atmospheric aerosols over the northwest Pacific Ocean, Atmos. Environ., 32, 1931–1946, 1998.

Matsumoto, K., Uyama, Y., Hayano, T., and Uematsu, M.: Transport and chemical transformation of anthropogenic and mineral aerosol in the marine boundary layer over the western North Pacific Ocean, J. Geophys. Res.-Atmos., 109, D21206, doi:10.1029/2004JD004696, 2004.

Matsumoto, K., Minami, H., Hayano, T., Uyama, Y., Tanimoto, H., and Uematsu, M.: Regional climatology of particulate carbonaceous substances in the northern area of the east Asian Pacific rim, J. Geophys. Res.-Atmos., 112, D24203, doi:10.1029/2007JD008607, 2007.

Title Page

Abstract | Introduction

Conclusions | References

Tables | Figures

|◄ | ►|

◄ | ►

Back | Close

Full Screen / Esc

Printer-friendly Version

Interactive Discussion

Mihalopoulos, N., Nguyen, B. C., Boissard, C., Campin, J. M., Putaud, J. P., Belviso, S., Barnes, I., and Becker, K. H.: Field study of dimethylsulfide oxidation in the boundary layer: variations of dimethylsulfide, methanesulfonic acid, sulfur dioxide, non-sea-salt sulfate and aitken nuclei at a coastal site, J. Atmos. Chem., 14, 459–477, doi:10.1007/BF00115251, 1992.

Miyazaki, Y., Fu, P. Q., Kawamura, K., Mizoguchi, Y., and Yamanoi, K.: Seasonal variations of stable carbon isotopic composition and biogenic tracer compounds of water-soluble organic aerosols in a deciduous forest, Atmos. Chem. Phys., 12, 1367–1376, doi:10.5194/acp-12-1367-2012, 2012.

Mochida, M., Kawabata, A., Kawamura, K., Hatsushika, H., and Yamazaki, K.: Seasonal variation and origins of dicarboxylic acids in the marine atmosphere over the western North Pacific, J. Geophys. Res.-Atmos., 108, 4193, doi:10.1029/2002JD002355, 2003.

Mochida, M., Kawamura, K., Fu, P., and Takemura, T.: Seasonal variation of levoglucosan in aerosols over the western North Pacific and its assessment as a biomass-burning tracer, Atmos. Environ., 44, 3511–3518, doi:10.1016/j.atmosenv.2010.06.017, 2010.

O'Dowd, C. D., Smith, M. H., Consterdine, I. E., and Lowe, J. A.: Marine aerosol, sea-salt, and the marine sulphur cycle: a short review, Atmos. Environ., 31, 73–80, 1997.

O'Dowd, C. D., Lowe, J. A., and Smith, M. H.: Coupling sea-salt and sulphate interactions and its impact on cloud droplet concentration predictions, Geophys. Res. Lett., 26, 1311–1314, 1999.

Pavuluri, C. M., Kawamura, K., Aggarwal, S. G., and Swaminathan, T.: Characteristics, seasonality and sources of carbonaceous and ionic components in the tropical aerosols from Indian region, Atmos. Chem. Phys., 11, 8215–8230, doi:10.5194/acp-11-8215-2011, 2011.

Pavuluri, C. M., Kawamura, K., Mihalopoulos, N., and Fu, P.: Year-round observations of water-soluble ionic species and trace metals in Sapporo aerosols: implication for significant contributions from terrestrial biological sources in Northeast Asia, Atmos. Chem. Phys. Discuss., 13, 6589–6629, doi:10.5194/acpd-13-6589-2013, 2013.

Quinn, P. K., Bates, T. S., Johnson, J. E., Covert, D. S., and Charlson, R. J.: Interactions between the sulfur and reduced nitrogen cycles over the central Pacific Ocean, J. Geophys. Res.-Atmos., 95, 16405–16416, doi:10.1029/JD095iD10p16405, 1990.

Quinn, P. K., Bates, T. S., Coffman, D. J., Miller, T. L., Johnson, J. E., Covert, D. S., Putaud, J. P., Neususs, C., and Novakov, T.: A comparison of aerosol chemical and optical properties from the 1st and 2nd Aerosol Characterization Experiments, Tellus B, 52, 239–257, 2000.

Title Page

Abstract | Introduction

Conclusions | References

Tables | Figures

Back | Close

Full Screen / Esc

Printer-friendly Version

Interactive Discussion

Ramanathan, V., Crutzen, P. J., Kiehl, J. T., and Rosenfeld, D.: Aerosols, climate, and the hydrological cycle, Science, 294, 2119–2124, 2001.

Ramos, A. G., Martel, A., Codd, G. A., Soler, E., Coca, J., Redondo, A., Morrison, L. F., Metcalf, J. S., Ojeda, A., Suarez, S., and Petit, M.: Bloom of the marine diazotrophic cyanobacterium *Trichodesmium erythraeum* in the northwest African upwelling, Mar. Ecol.-Prog. Ser., 301, 303–305, 2005.

Rudich, Y., Khersonsky, O., and Rosenfeld, D.: Treating clouds with a grain of salt, Geophys. Res. Lett., 29, 2064, doi:10.1029/2002GL016055, 2002.

Satheesh, S. K. and Krishna Moorthy, K.: Radiative effects of natural aerosols: a review, Atmos. Environ., 39, 2089–2110, doi:10.1016/j.atmosenv.2004.12.029, 2005.

Savoie, D. L. and Prospero, J. M.: Comparison of oceanic and continental sources of non-sea-salt sulphate over the Pacific Ocean, Nature, 339, 685–687, 1989.

Sullivan, R. C. and Prather, K. A.: Investigations of the diurnal cycle and mixing state of oxalic acid in individual particles in Asian aerosol outflow, Environ. Sci. Technol., 41, 8062–8069, doi:10.1021/es071134g, 2007.

Sun, J., Zhang, M., and Liu, T.: Spatial and temporal characteristics of dust storms in China and its surrounding regions, 1960–1999: relations to source area and climate, J. Geophys. Res.-Atmos., 106, 10325–10333, doi:10.1029/2000JD900665, 2001.

Suzuki, I., Hayashi, K., Igarashi, Y., Takahashi, H., Sawa, Y., Ogura, N., Akagi, T., and Dokiya, Y.: Seasonal variation of water-soluble ion species in the atmospheric aerosols at the summit of Mt. Fuji, Atmos. Environ., 42, 8027–8035, doi:10.1016/j.atmosenv.2008.06.014, 2008.

Tang, I. N., Tridico, A. C., and Fung, K. H.: Thermodynamics and optical properties of sea salt aerosols, J. Geophys. Res., 102, 23269–23275, 1997.

Twomey, S.: Influence of pollution on shortwave albedo of clouds, J. Atmos. Sci., 34, 1149–1152, 1977.

Uematsu, M., Sugita, T., Anikiev, V. V., and Medvedev, A. N.: Large-scale transport of pollution aerosol over the east coast of Asia, Geophys. Res. Lett., 19, 2219–2221, doi:10.1029/92GL02639, 1992.

Woodcock, A. H.: Salt nuclei in marine air as a function of attitude and wind force, J. Meterol., 10, 362–371, 1953.

Wu, D., Tie, X., and Deng, X.: Chemical characterizations of soluble aerosols in southern China, Chemosphere, 64, 749–757, doi:10.1016/j.chemosphere.2005.11.066, 2006.

Title Page

Abstract | Introduction

Conclusions | References

Tables | Figures

|◄ | ►|

◄ | ►

Back | Close

Full Screen / Esc

Printer-friendly Version

Interactive Discussion

Yin, F., Grosjean, D., Flagan, R., and Seinfeld, J.: Photooxidation of dimethyl sulfide and dimethyl disulfide. II: Mechanism evaluation, J. Atmos. Chem., 11, 365–399, doi:10.1007/BF00053781, 1990.

Zhang, T., Cao, J. J., Tie, X. X., Shen, Z. X., Liu, S. X., Ding, H., Han, Y. M., Wang, G. H., Ho, K. F., Qiang, J., and Li, W. T.: Water-soluble ions in atmospheric aerosols measured in Xi'an, China: seasonal variations and sources, Atmos. Res., 102, 110–119, doi:10.1016/j.atmosres.2011.06.014, 2011.

A 12 year observation of water-soluble inorganic ions in TSP aerosols

S. K. R. Boreddy and K. Kawamura

Title Page

Abstract	Introduction
Conclusions	References
Tables	Figures

|◄ ►|

◄ ►

Back Close

Full Screen / Esc

Printer-friendly Version

Interactive Discussion

Table 1. Seasonal mean concentrations (μg^{-3}) of major inorganic ions (mean ± SD) with two tailed P value at Chichijima Island during 2001–2012.

	MSA^-	Cl^-	NO_3^-	$Nss\text{-}SO_4^{2-}$	Na^+	NH_4^+	$Nss\text{-}K^+$	$Nss\text{-}Ca^{2+}$	Mg^{2+}
Winter	0.02 ± 0.00	7.10 ± 0.88	0.78 ± 0.14	3.06 ± 0.43	4.12 ± 0.47	0.19 ± 0.06	0.05 ± 0.03	0.12 ± 0.03	0.48 ± 0.05
Spring	0.03 ± 0.01	6.18 ± 1.20	0.84 ± 0.15	2.97 ± 0.89	3.32 ± 0.59	0.23 ± 0.10	0.05 ± 0.02	0.30 ± 0.12	0.42 ± 0.07
Summer	0.02 ± 0.00	4.94 ± 1.54	0.24 ± 0.09	1.06 ± 0.59	2.52 ± 0.71	0.11 ± 0.13	0.02 ± 0.01	0.04 ± 0.04	0.29 ± 0.09
Autumn	0.01 ± 0.00	7.12 ± 2.61	0.43 ± 0.11	1.31 ± 0.42	3.62 ± 1.06	0.11 ± 0.05	0.05 ± 0.04	0.04 ± 0.03	0.40 ± 0.11
P value	< 0.001	< 0.001	< 0.001	< 0.001	< 0.001	< 0.001	< 0.001	< 0.001	< 0.001

Table 2. Annual mean concentrations (μg^{-3}) of major inorganic ions (mean ± SD) with two tailed P value during 2001–2012 at Chichijima Island.

	MSA^-	Cl^-	NO_3^-	$Nss\text{-}SO_4^{2-}$	Na^+	NH_4^+	$Nss\text{-}K^+$	$Nss\text{-}Ca^{2+}$	Mg^{2+}
2001	0.01 ± 0.00	5.65 ± 2.82	0.47 ± 0.29	1.67 ± 1.11	2.87 ± 1.36	0.09 ± 0.04	0.03 ± 0.01	0.15 ± 0.19	0.33 ± 0.16
2002	0.02 ± 0.01	6.84 ± 2.66	0.61 ± 0.41	2.81 ± 1.66	3.59 ± 1.20	0.27 ± 0.17	0.05 ± 0.03	0.18 ± 0.26	0.44 ± 0.15
2003	0.02 ± 0.01	7.23 ± 2.16	0.60 ± 0.36	2.17 ± 1.21	3.85 ± 1.19	0.13 ± 0.07	0.05 ± 0.03	0.10 ± 0.11	0.45 ± 0.15
2004	0.02 ± 0.01	8.41 ± 4.14	0.54 ± 0.39	2.27 ± 1.65	4.46 ± 1.42	0.16 ± 0.07	0.06 ± 0.04	0.08 ± 0.08	0.50 ± 0.16
2005	0.02 ± 0.00	7.25 ± 2.24	0.69 ± 0.40	2.32 ± 1.24	4.12 ± 1.03	0.10 ± 0.07	0.04 ± 0.01	0.11 ± 0.10	0.46 ± 0.13
2006	0.02 ± 0.01	6.58 ± 2.56	0.64 ± 0.43	2.20 ± 1.56	3.58 ± 1.07	0.14 ± 0.15	0.03 ± 0.03	0.16 ± 0.23	0.41 ± 0.14
2007	0.02 ± 0.01	5.63 ± 1.51	0.67 ± 0.35	2.77 ± 1.39	3.36 ± 1.01	0.36 ± 0.32	0.07 ± 0.04	0.17 ± 0.15	0.39 ± 0.13
2008	0.02 ± 0.01	4.83 ± 2.35	0.49 ± 0.29	2.28 ± 1.42	2.89 ± 1.12	0.16 ± 0.11	0.08 ± 0.06	0.08 ± 0.09	0.33 ± 0.13
2009	0.03 ± 0.01	6.46 ± 2.64	0.57 ± 0.37	1.51 ± 1.18	3.47 ± 1.03	0.13 ± 0.08	0.03 ± 0.02	0.09 ± 0.08	0.40 ± 0.11
2010	0.02 ± 0.01	5.15 ± 2.31	0.55 ± 0.38	1.71 ± 1.19	2.71 ± 1.25	0.15 ± 0.14	0.03 ± 0.02	0.15 ± 0.20	0.32 ± 0.15
2011	0.02 ± 0.01	5.56 ± 1.51	0.51 ± 0.31	1.67 ± 1.34	2.85 ± 0.81	0.14 ± 0.15	0.03 ± 0.04	0.10 ± 0.13	0.34 ± 0.11
2012	0.02 ± 0.01	7.04 ± 1.87	0.64 ± 0.51	2.03 ± 1.43	3.49 ± 0.97	0.18 ± 0.18	0.04 ± 0.02	0.15 ± 0.15	0.43 ± 0.12
Mean	0.02 ± 0.00	6.39 ± 1.04	0.58 ± 0.07	2.12 ± 0.42	3.44 ± 0.54	0.17 ± 0.07	0.05 ± 0.01	0.13 ± 0.03	0.40 ± 0.05
P value	< 0.001	< 0.001	< 0.001	< 0.001	< 0.001	< 0.001	< 0.001	< 0.001	< 0.001

Table 3. Correlation coefficient matrix among the major chemical species for different seasons during 2001–2012.

	MSA^-	Cl^-	NO_3^-	SO_4^{2-}	Na^+	Winter NH_4^+	K^+	Ca^{2+}	Mg^{2+}	$nss\text{-}SO_4^{2-}$	$nss\text{-}K^+$	$nss\text{-}Ca^{2+}$
MSA^-	1											
Cl^-	−0.199(*)	1										
NO_3^-	0.365(**)	−0.166	1									
SO_4^{2-}	0.481(**)	−0.125	0.689(**)	1								
Na^+	−0.011	0.876(**)	0.209(*)	0.261(**)	1							
NH_4^+	0.562(**)	−0.261(**)	0.622(**)	0.821(**)	0.081	1						
K^+	0.446(**)	0.281(**)	0.568(**)	0.759(**)	0.561(**)	0.744(**)	1					
Ca^{2+}	0.303(**)	0.347(**)	0.513(**)	0.478(**)	0.524(**)	0.372(**)	0.533(**)	1				
Mg^{2+}	0.060	0.848(**)	0.240(**)	0.291(**)	0.966(**)	0.124	0.589(**)	0.545(**)	1			
$nss\text{-}SO_4^{2-}$	0.496(**)	−0.262(**)	0.677(**)	0.989(**)	0.116	0.835(**)	0.696(**)	0.412(**)	0.153	1		
$nss\text{-}K^+$	0.520(**)	−0.155	0.518(**)	0.748(**)	0.107	0.829(**)	0.879(**)	0.338(**)	0.149	0.755(**)	1	
$nss\text{-}Ca^{2+}$	0.343(**)	0.052	0.480(**)	0.420(**)	0.195(*)	0.380(**)	0.373(**)	0.936(**)	0.229(*)	0.404(**)	0.338(**)	1

	MSA^-	Cl^-	NO_3^-	SO_4^{2-}	Na^+	Spring NH_4^+	K^+	Ca^{2+}	Mg^{2+}	$nss\text{-}SO_4^{2-}$	$nss\text{-}K^+$	$nss\text{-}Ca^{2+}$
MSA^-	1											
Cl^-	0.199(*)	1										
NO_3^-	0.388(**)	0.240(**)	1									
SO_4^{2-}	0.349(**)	0.089	0.619(**)	1								
Na^+	0.258(**)	0.888(**)	0.418(**)	0.467(**)	1							
NH_4^+	0.368(**)	−0.150	0.504(**)	0.710(**)	0.026	1						
K^+	0.305(**)	0.416(**)	0.703(**)	0.710(**)	0.639(**)	0.474(**)	1					
Ca^{2+}	0.236(**)	0.353(**)	0.665(**)	0.485(**)	0.355(**)	0.258(**)	0.516(**)	1				
Mg^{2+}	0.382(**)	0.872(**)	0.519(**)	0.416(**)	0.912(**)	0.105	0.660(**)	0.545(**)	1			
$nss\text{-}SO_4^{2-}$	0.418(**)	−0.008	0.609(**)	0.988(**)	0.456(**)	0.770(**)	0.646(**)	0.473(**)	0.362(**)	1		
$nss\text{-}K^+$	0.294(**)	−0.082	0.539(**)	0.578(**)	0.034	0.631(**)	0.655(**)	0.360(**)	0.137	0.611(**)	1	
$nss\text{-}Ca^{2+}$	0.200(*)	0.220(**)	0.621(**)	0.440(**)	0.200(*)	0.256(**)	0.421(**)	0.988(**)	0.404(**)	0.444(**)	0.369(**)	1

Title Page

Abstract | Introduction

Conclusions | References

Tables | Figures

|◄ | ►|

◄ | ►

Back | Close

Full Screen / Esc

Printer-friendly Version

Interactive Discussion

Table 3. Continued.

	MSA$^-$	Cl$^-$	NO$_3^-$	SO$_4^{2-}$	Na$^+$	NH$_4^+$	K$^+$	Ca^{2+}	Mg^{2+}	nss-SO$_4^{2-}$	nss-K$^+$	nss-Ca^{2+}
						Summer						
MSA$^-$	1											
Cl$^-$	−0.163	1										
NO$_3^-$	0.422(**)	−0.161	1									
SO$_4^{2-}$	0.425(**)	0.029	0.376(**)	1								
Na$^+$	−0.065	0.949(**)	−0.049	0.192(*)	1							
NH$_4^+$	0.359(**)	−0.243	0.485(**)	0.866(**)	−0.096	1						
K$^+$	0.123	0.811(**)	0.062	0.429(**)	0.862(**)	0.513(**)	1					
Ca^{2+}	0.127	0.765(**)	0.148	0.258(**)	0.797(**)	0.195	0.776(**)	1				
Mg^{2+}	−0.027	0.939(**)	−0.009	0.202(*)	0.980(**)	−0.046	0.885(**)	0.817(**)	1			
nss-SO$_4^{2-}$	0.535(**)	−0.200(*)	0.455(**)	0.968(**)		0.911(**)	0.242(**)	0.082	−0.039	1		
nss-K$^+$	0.376(**)	−0.067	0.471(**)	0.666(**)	−0.007	0.876(**)	0.456(**)	0.212	0.053	0.738(**)	1	
nss-Ca^{2+}	0.277(**)	0.006	0.259(**)	0.147	−0.016	0.384(**)	0.151	0.601(**)	0.045	0.213(*)	0.266(*)	1

|	MSA$^-$	Cl$^-$	NO$_3^-$	SO$_4^{2-}$	Na$^+$	NH$_4^+$	K$^+$	Ca^{2+}	Mg^{2+}	nss-SO$_4^{2-}$	nss-K$^+$	nss-Ca^{2+}
						Autumn						
MSA$^-$	1											
Cl$^-$	0.007	1										
NO$_3^-$	0.517(**)	0.037	1									
SO$_4^{2-}$	0.554(**)	0.104	0.753(**)	1								
Na$^+$	0.249(**)	0.925(**)	0.338(**)	0.217(**)	1							
NH$_4^+$	0.342(**)	−0.131	0.360(**)	0.463(**)	0.088	1						
K$^+$	0.410(**)	0.567(**)	0.582(**)	0.734(**)	0.754(**)	0.529(**)	1					
Ca^{2+}	0.292(**)	0.505(**)	0.492(**)	0.584(**)	0.629(**)	0.336(**)	0.653(**)	1				
Mg^{2+}	0.274(**)	0.895(**)	0.428(**)	0.485(**)	0.970(**)	0.122	0.807(**)	0.637(**)	1			
nss-SO$_4^{2-}$	0.583(**)	−0.111	0.760(**)	0.970(**)	0.224(**)	0.610(**)	0.626(**)	0.483(**)	0.310(**)	1		
nss-K$^+$	0.359(**)	−0.137	0.432(**)	0.667(**)	0.189	0.828(**)	0.738(**)	0.531(**)	0.230	0.699(**)	1	
nss-Ca^{2+}	0.163	0.075	0.364(**)	0.442(**)	0.170	0.477(**)	0.343(**)	0.879(**)	0.180	0.434(**)	0.623(**)	1

[**] Correlation is significant at the 0.01 level (2-tailed).
[*] Correlation is significant at the 0.05 level (2-tailed).
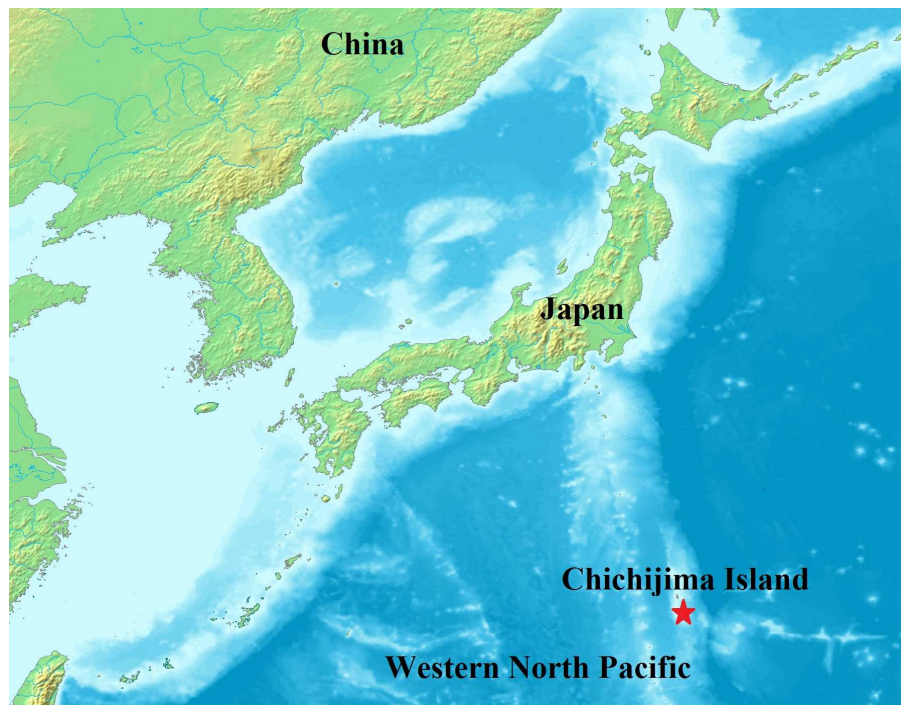
Figure 1. The geographical location of Chichijima Island (indicated by red colored star) in the western North Pacific.

Longitude °E
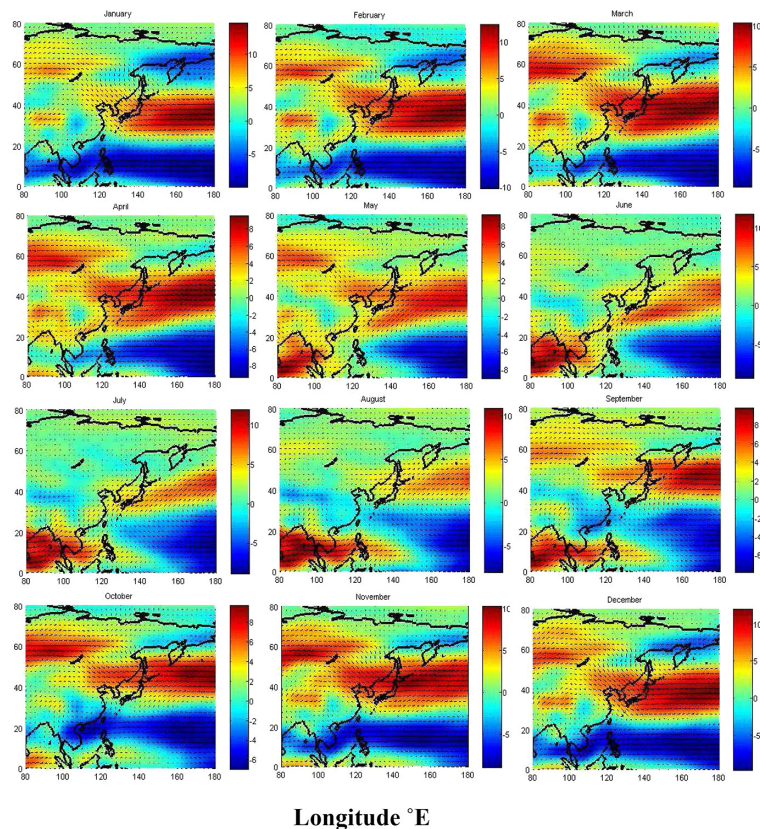
Figure 2. NCEP/NCAR reanalysis of Mean synoptic wind vector ($\mathrm{m\,s^{-1}}$) at 850 mb pressure level for each month over the study area during 2001–2012.
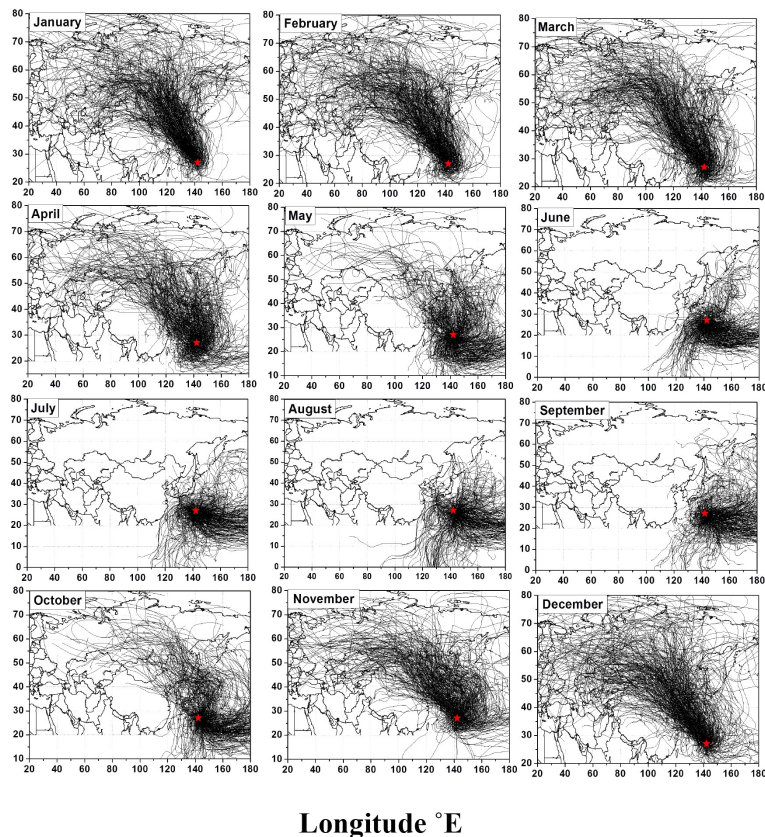
Longitude ˚E

Figure 3. NOAA HYSPLIT 10 day backward air mass trajectories at 500 m a.g.l. for each month over Chichijima Island during 2001–2012.
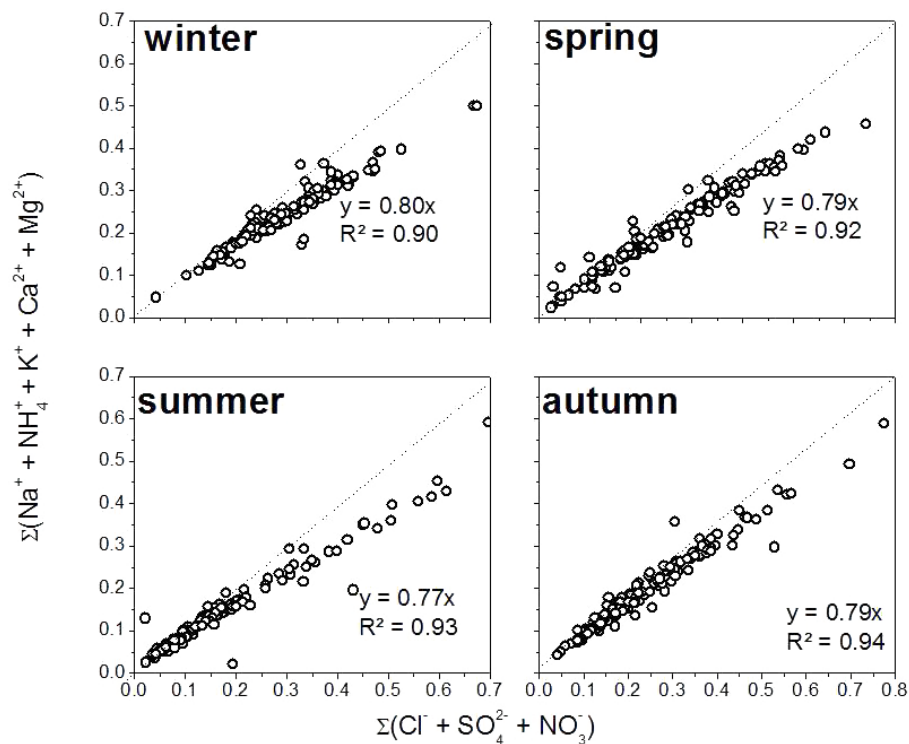
Figure 4. Charge Balance of ions ($\mu eq\,m^{-3}$) on a seasonal scale.
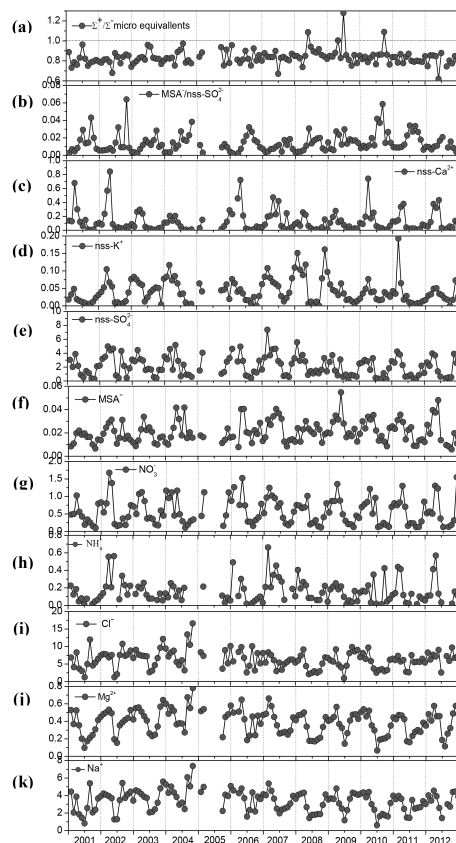
Figure 5. Temporal variations of different measured/derivec inorganic ions ($\mu g\,m^{-3}$) and mass ratios over the western North Pacific during 2001–2012. Each data point represents month in the each year.
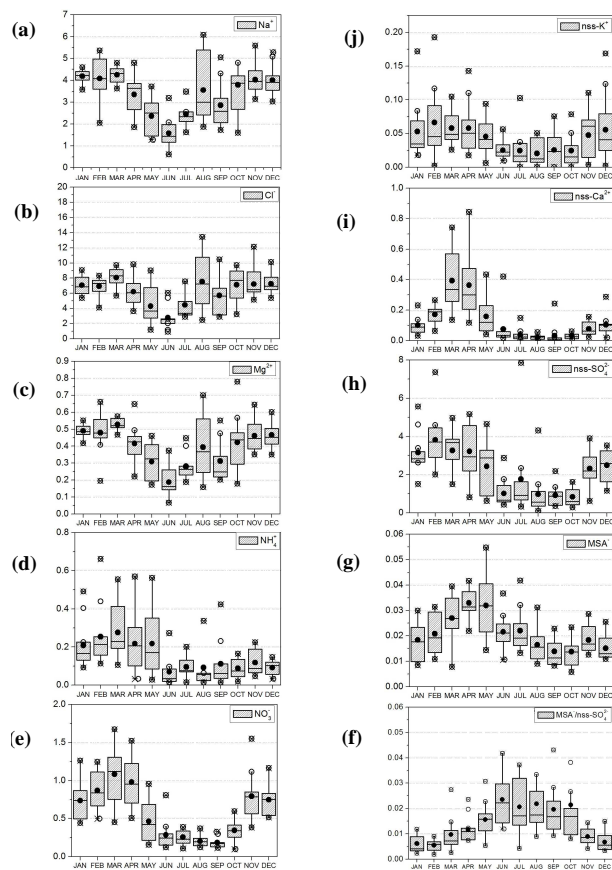
Figure 6. Box–Whisker plot of monthly variations of different measured/derived inorganic species ($\mu g\,m^{-3}$) and mass ratio for the period 2001–2012 over the western North Pacific.

Title Page

Abstract | Introduction

Conclusions | References

Tables | Figures

|◄ | ►|

◄ | ►

Back | Close
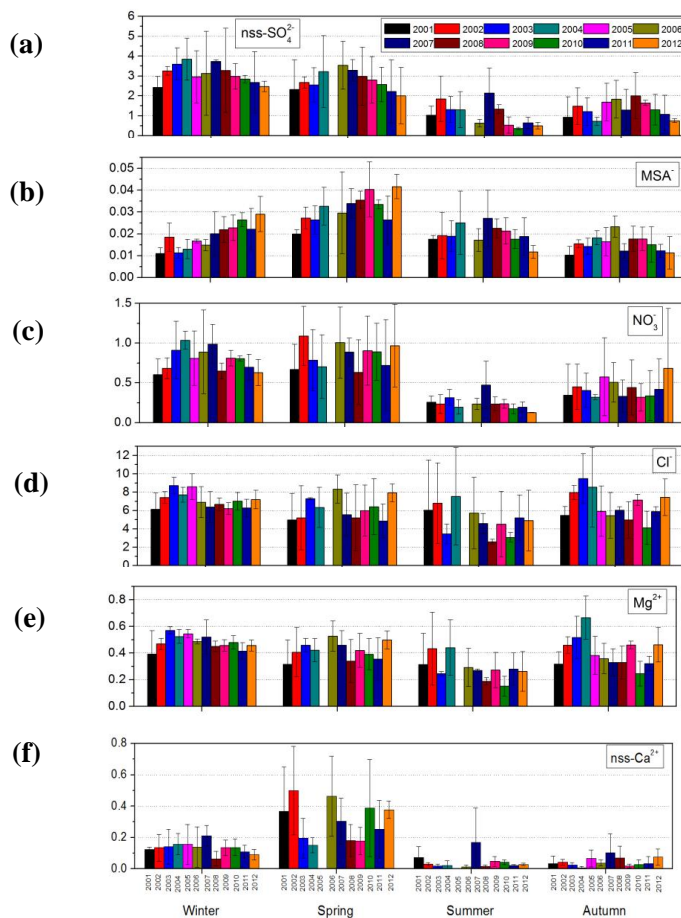
Full Screen / Esc

Figure 7. Annual variations of different chemical species (μg m^{-3}) on a seasonal scale over the sampling period of 2001–2012.
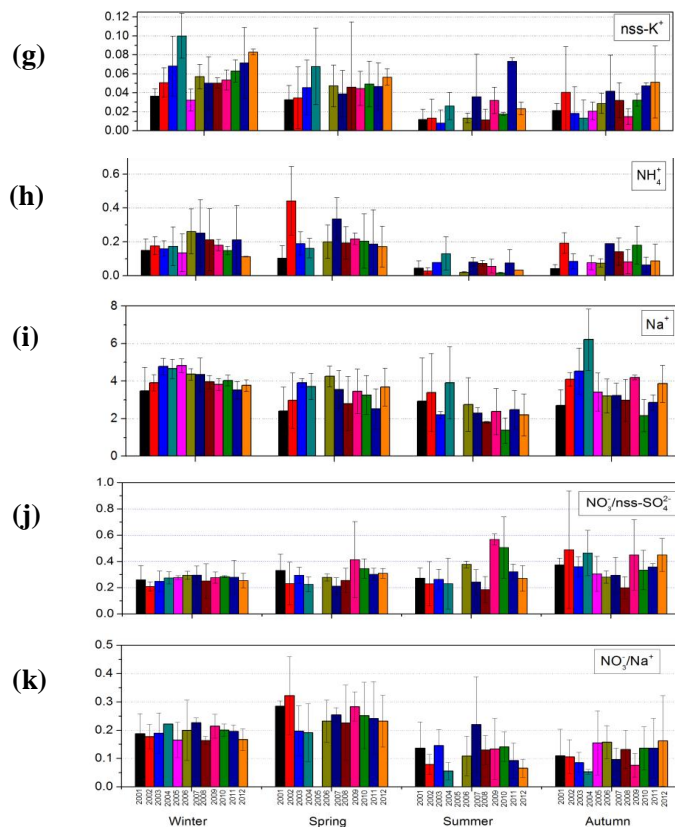
Figure 7. Continued.

Title Page

Abstract | Introduction

Conclusions | References

Tables | Figures

|◀ | ▶|

◀ | ▶

Back | Close

Full Screen / Esc

Printer-friendly Version

Interactive Discussion
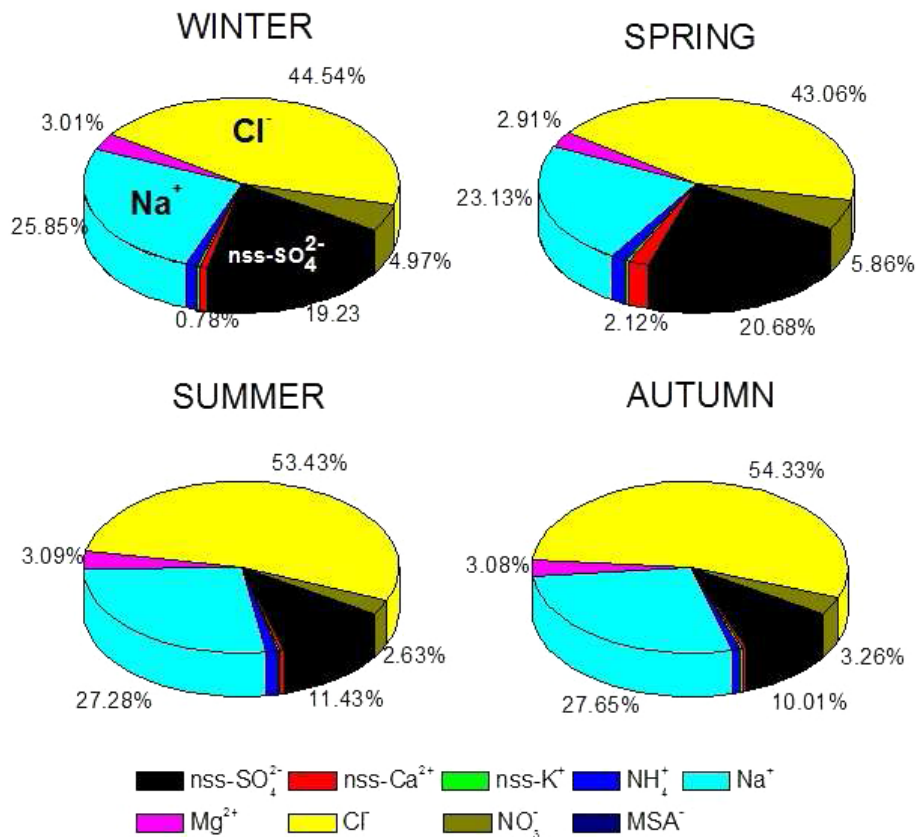
Figure 8. Percentage contribution of major ions to total water-soluble inorganic ions for different seasons.

Title Page

Abstract | Introduction

Conclusions | References

Tables | Figures

|◄ | ►|

◄ | ►

Back | Close

Full Screen / Esc

Printer-friendly Version

Interactive Discussion
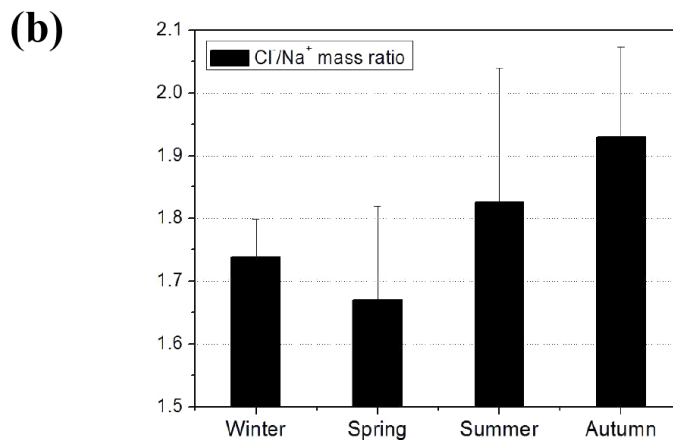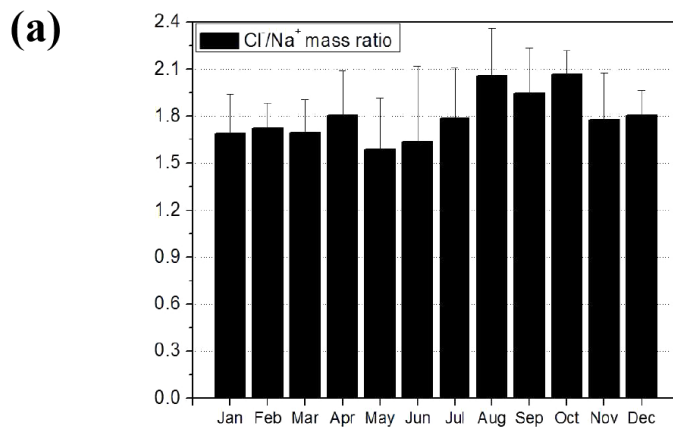
Figure 9. Variation of Cl⁻/Na⁺ mass ratio on **(a)** monthly **(b)** seasonal scales.
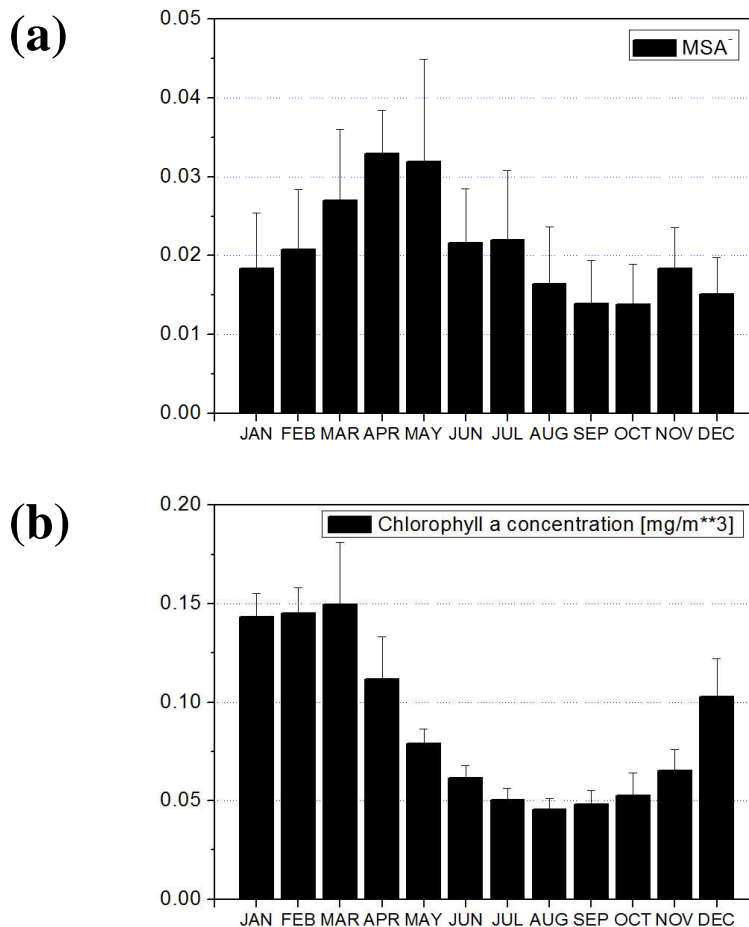
Figure 10. Monthly mean variation of **(a)** MSA$^-$ ($\mu g\,m^{-3}$) **(b)** chlorophyll *a* concentrations for the study period. Chlorophyll *a* concentrations were downloaded from MODIS AQUA satellite over the region (140–145° E, 25–30° N) for the study period.